



**HAL**  
open science

## Transition to turbulence in globally subcritical systems

Paul Manneville, J. Rolland

► **To cite this version:**

Paul Manneville, J. Rolland. Transition to turbulence in globally subcritical systems. CFM 2009 - 19ème Congrès Français de Mécanique, Aug 2009, Marseille, France. pp.S9 Instabilités et Transition, Contrôle d'Écoulement. hal-01053078

**HAL Id: hal-01053078**

**<https://polytechnique.hal.science/hal-01053078>**

Submitted on 29 Jul 2014

**HAL** is a multi-disciplinary open access archive for the deposit and dissemination of scientific research documents, whether they are published or not. The documents may come from teaching and research institutions in France or abroad, or from public or private research centers.

L'archive ouverte pluridisciplinaire **HAL**, est destinée au dépôt et à la diffusion de documents scientifiques de niveau recherche, publiés ou non, émanant des établissements d'enseignement et de recherche français ou étrangers, des laboratoires publics ou privés.

# Transition to turbulence in globally subcritical systems

P. MANNEVILLE<sup>a</sup>, J. ROLLAND<sup>a,b</sup>

*a. LadHyX, École Polytechnique, 91128 PALAISEAU*

*b. École Normale Supérieure, rue d'Ulm, 75005 PARIS*

## Résumé :

*Prenant l'exemple de l'écoulement de Couette plan, nous discutons l'état actuel de notre compréhension de la transition vers la turbulence dans les systèmes globalement sous-critiques, et notamment des particularités des parties basse et haute de la région de transition.*

## Abstract :

*Taking the example of plane Couette flow, we discuss our current understanding of the transition to turbulence in globally subcritical systems, pointing out the specificity of the lower and upper parts of the transitional range.*

**Mots clefs :** transition to turbulence, subcritical systems, plane Couette flow

## 1 General setting

Understanding the transition to turbulence in flows lacking linear instability modes, such as Poiseuille pipe flow (PPF) and plane Couette flow (PCF), is particularly challenging in view of its direct character, without the usual cascade seen in the “globally supercritical” case as for, e.g., convection. These “globally subcritical” flows become turbulent through the nucleation and growth or decay of turbulent domains called puffs (PPF) or spots (PCF). Such states have been interpreted within the framework of dynamical systems theory as transient chaotic states associated to stochastic repellers [1]. Though this can explain the exponentially decreasing distribution of the transient lifetimes, the story is still incomplete since it does not say how the exponential decrement should vary with the control parameter, the Reynolds number  $R$ , and whether or not there exists a critical value  $R_g$  above which turbulence is sustained, which has been the subject of hot debates, at least for PPF [2, 3], but also for PCF [4, 5]. Long ago, Pomeau [6] conjectured that such transitions should be akin to directed percolation, a stochastic process studied in statistical physics. He also proposed a connection with first-order thermodynamic phase transitions and their associated nucleation properties. This viewpoint shifts the focus from the theory of low-dimensional dynamical systems and temporal chaos to the field of statistical physics and spatiotemporal chaos. It motivated what will be presented in Section 2 below.

Fig. 1 illustrates the bifurcation diagram of PCF with  $R = \bar{U}h/\nu$ , where  $U$  is the speed of the plates driving the flow,  $2h$  the distance between them, and  $\nu$  the kinematic viscosity of the fluid. (A definition based on the average shear,  $\tilde{R} = (U/d)(2d)^2/\nu = 4R$ , would be more appropriate to make meaningful comparisons with PPF or counter-rotating Taylor-Couette flow.)

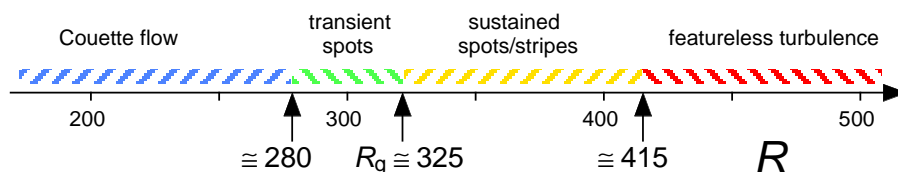


FIG. 1 – Bifurcation diagram in the case of PCF, as compiled from the work done at Saclay.

In both PPF and PCF, the transitional regime extends over a rather wide domain of  $R$  and one has to distinguish the lower part from the upper part of this range. In the lower part, inhomogeneity prevails, puffs/spots coexisting with laminar flow, and the dynamics is basically controlled by the fact that locally turbulent flow can decay to laminar flow. On the other hand, the upper part is characterised by the fact that turbulent patches tend to gain over the laminar flow, i.e., puffs of limited extent transform themselves into ever growing turbulent slugs in PPF, and turbulent spots align to form oblique bands with the turbulent intensity becoming more and more uniform as  $R$  increases in PCF. Experimentally, the upper transitional regime is better documented for PCF

than for PPF, because it can be studied in the cylindrical Taylor–Couette configuration with marginal role of the curvature in exact counter-rotation [7, 8].

## 2 A spatiotemporal perspective on the decay of turbulence in PCF.

On the one hand, a large body of information on the transitional regime in PPF and PCF comes from numerical simulations in small size domains with periodic boundary conditions at short distances, comparable to the pipe’s diameter [9] or the distance between the plates [10]. The analysis of the results nicely fit the framework of the theory of low-dimensional dissipative dynamical systems but the latter fails to account for the fact that experiments are done in quasi-1D (PPF) or quasi-2D (PCF) systems. For PCF, computing power just begins to be sufficient to deal with numerical simulations in domains of sizes relevant to experiments [11, 12]. An exception is the quasi-1D study of Barkley & Tuckerman [13, 14] to be alluded to later, more meaningful than the quasi-0D dynamical systems framework, though with unclear implications in a fully quasi-2D context.

On the other hand, previous modelling of spatiotemporal chaos in PCF was performed in the abstract setting of coupled map lattices with limited success [15]. A few years later, more realistic modelling began to be developed using a standard Galerkin method applied to the Navier–Stokes equations (NSE). A small number of modes was kept in the cross-stream direction but the in-plane functional dependence was accounted for, without more approximation than what resulted from the cross-stream truncation. Stress-free plates [16] were considered first, but the model was next extended to deal with the no-slip case [17]. The reduced cross-stream resolution allowed us to consider simulation domains of sizes of the order of those of experimental set-ups, i.e. much larger than those that could be considered with conventional direct simulation aiming at a quantitative account of the evolution. Experiments showed that, once reduced to only three two-dimensional fields, two stream functions and one velocity potential (governing equations are given in the appendix), the model retained the most significant qualitative characteristics of transitional Couette flow, namely the specific couplings involved in the self-sustaining turbulence mechanism [18] and the sub-critical nature of the transition from laminar to turbulent flow. The price to be paid was a lowering by a factor of 2 of the transitional Reynolds numbers, due to severe underestimation of energy transfer and viscous dissipation through the cross-stream small scales. The positive side was that very wide domains could be considered and computations could be performed during very long periods of time, thus allowing one to approach the “thermodynamic limit” in the sense of statistical physics.

Simulations reported here have been performed on a domain of size  $\mathcal{D} = 1536 \times 2 \times 1536$ ,<sup>1</sup> by decreasing  $R$  adiabatically from a fully turbulent regime at  $R = 200$  [20]. The solution followed in that way turned out to remain turbulent down to  $R \sim 171.5$  but decayed irreversibly to laminar flow for  $R = 171$ . See Fig. 2 (top-left, and bottom).

The flow patterns were statistically analysed by first defining a robust criterion identifying laminar domains with perturbation energy smaller than some empirically determined threshold, next determining the probability distribution of the laminar domain sizes (Fig. 2, top-right). Let  $\Pi(S)$  be the probability distribution functions of the surface  $S$  of the laminar domains immersed in the turbulent sea. To a good approximation, their large- $S$  tails behave as power laws,  $\Pi(S) \sim S^{-\alpha}$ . The average surface occupied by the laminar domains is given by  $\int_{S_*}^{\infty} S\Pi(S)dS$  and the second moment by  $\int_{S_*}^{\infty} S^2\Pi(S)dS$ . Values of  $\alpha$  reported in Fig. 2 (top-right) are close to 3. When  $\alpha > 3$ , the average laminar surface and the second moment, hence the variance, are all finite. On the contrary, when  $\alpha < 3$ , the average remains finite but the variance diverge. The first situation holds at  $R = 171.5$  and the second at  $R = 171$ . These facts have to be interpreted within the framework of nucleation theory : on general grounds, the turbulent state can decay only if a germ beyond some critical size appears in the system. So, the system adiabatically brought at  $R = 171.5$  does not decay because the critical germ size is presumably much larger than the variance of the distribution of laminar domain sizes, which implies a negligible probability of occurrence of a critical germ. On the contrary, in the same conditions, the system at  $R = 171$  will sooner or later decay because the variance of the distribution diverges, making the occurrence of a critical germ certain. This argument proves the existence of a genuine transition at the thermodynamic limit [20]. In smaller systems, this specific spatiotemporal behaviour is masked by size effects, which justifies that in domains of size  $32 \times 2 \times 32$  a sharp transition is not observed, while chaotic transients are obtained with exponentially distributed lifetimes [17]. It is also important to notice that the argument does not forbid turbulent decay for  $R > 171.5$  but simply that the perturbation brought to the turbulent solution by a small decrease of  $R$  is sufficiently tiny to keep it inside the attraction basin of the turbulent state which, though probably quite narrow, has still a finite measure. Larger perturbations, in particular those produced by large a quench from high  $R$  can trigger the decay. In contrast, for  $R \sim 171$  the turbulent state has presumably turned to a repeller with inset of measure 0.

To conclude this part, let us notice that the approach has the merit to suggest an alternative interpretation of the transition to turbulence that does not rely on the fact that the lifetime of chaos at a local scale has to diverge before turbulence can set in. Couplings implied by the physical space dependence are able to convert transient local chaos into sustained spatiotemporal chaos (turbulence) at some well defined Reynolds number in the middle of the transitional regime, which might be of consequence for PPF also in view of the controversy

<sup>1</sup>Experiments at GIT-Saclay were performed in systems of size ranging from  $380 \times 2 \times 70$  [5] to  $770 \times 2 \times 340$  [7]. It should be kept in mind that the most active small scale structures in the flow are of order  $6 \times 2 \times 3$  [19].

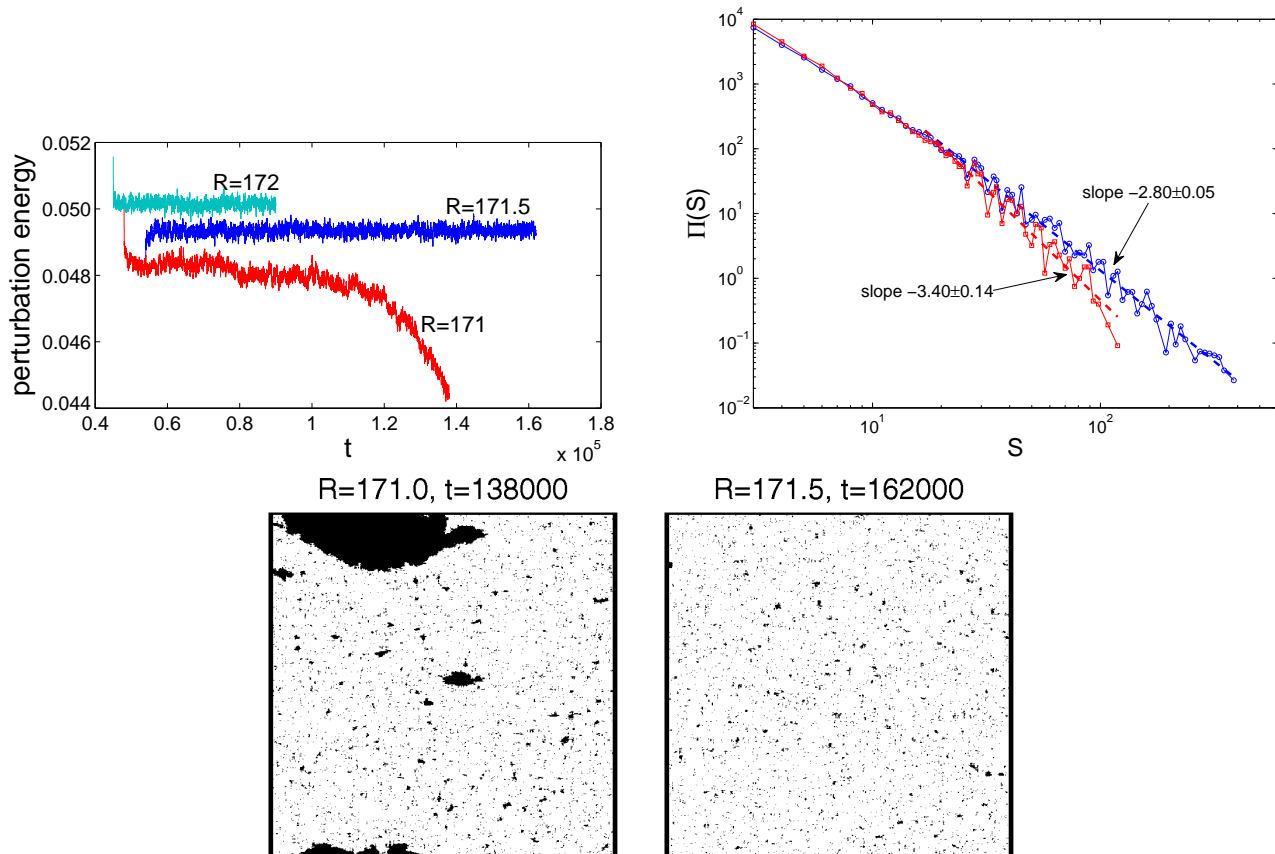


FIG. 2 – Top, left : Time series of the energy contained in the perturbation for several values of  $R$ . At  $t = 5 \times 10^4$   $R$  was reduced from 172 to 171 and the solution started to decay by nucleating a large laminar domain at  $t \simeq 8 \times 10^4$ . The state at  $t = 5.8 \times 10^4$  served as an initial condition for the experiment with  $R = 171.5$  which gave no sign of decay. Top, right : Probability distribution function  $\Pi(S)$  of the laminar domain size  $S$  for  $R = 171.5$  and  $R = 171$ . Bottom left : For  $R = 171$ , the laminar domain (black) that appeared at  $t \simeq 8 \times 10^4$  invaded the whole system. Several other large laminar domains were also scattered over the turbulent sea (white). Bottom right : For  $R = 171.5$  no large laminar domain is present and the subsequent analysis illustrated above (top-right) shows that the occurrence of such a large domain is unlikely.

about the very existence of sustained turbulence in that flow [2, 3].

### 3 Upper transitional regime in PCF

As already mentioned, the upper part of the transitional range in PCF is marked by the presence of oblique turbulent bands. When coming from the featureless turbulent regime, the formation of these bands appears to be a continuous process with turbulent intensity modulation increasing regularly as  $R$  is decreased below about  $R_t \simeq 415$  as illustrated in Fig. 3. A phenomenological description was proposed in terms of a stochastic 2-wave CGL model [8]

$$\tau_0(\partial_t \pm s_0 \partial_z)A_{\pm} = \epsilon A_{\pm} + \xi_0^2(1 + ic_1)\partial_{zz}A_{\pm} - g_3(1 - ic_3)|A_{\pm}|^2A_{\pm} - g'_3(1 - ic'_3)|A_{\mp}|^2A_{\pm} + \alpha\eta_{\pm}$$

where the noise term  $\eta$  was supposed to account for background turbulence. Coefficients of these equations could be fitted against experiments, yielding good overall interpretation of defects in the oblique band pattern and the turbulent intensity anomaly visible in Fig. 3 right, close to the featureless turbulence threshold [7, 8]. The phenomenon was also reproduced in the Barkley-Tuckerman (B&T, [13, 14]) numerical experiments specially designed to deal with the oblique band regime : they considered elongated (mostly spanwise) domains transversal to the bands but periodically repeated at a short distance in the (mostly streamwise) perpendicular direction. This approach gave insight into the structure of the flow, describing the average laminar-turbulent modulation by means of a few coupled sinusoidal terms [14] closely related to the large scale part of the in-plane modes introduced in our simplified Galerkin model [21].

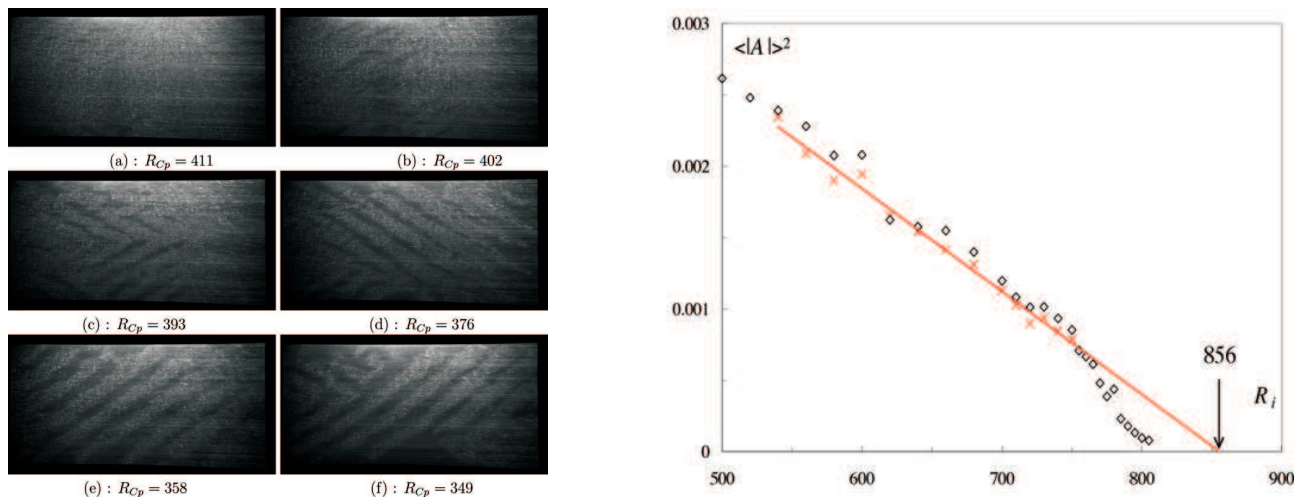


FIG. 3 – Left : Experimental observation of the emergence of oblique turbulent bands in PCF as  $R$  is decreased. Right : variation of the turbulent intensity modulation as a function of  $R$ , here for spiral bands in the upper transitional range of counter-rotating Taylor–Couette flow ( $R_i$  is the Reynolds number constructed with the radius and speed of the inner cylinder). From Prigent’s thesis [7].

Up to now, there is no theoretical understanding of the oblique turbulent intensity modulation. Despite its appealing features, our lowest-order model is unable to reproduce them systematically at large aspect ratio owing to its poor cross-stream resolution which forbids a reliable account of the upper transitional regime. Truncating the Galerkin expansion at higher orders could do the job but leads to increasingly cumbersome models which lose much their interest with respect to direct numerical simulations of the NSE. This is the reason why we are currently working at full 3D simulations<sup>2</sup> with lowered but controlled spatial resolution in spatially extended domains.

As a preliminary attempt, using Gibson’s public domain program CHANNELFLOW [22], we have performed the same experiment as in [17] in moderate aspect ratio systems of size  $128 \times 2 \times 64$  and  $64 \times 2 \times 128$ . Adiabatic decrease of  $R$  down from 450 led us to observe the oblique band regime in the same  $R$ -range as in the laboratory [7], see Fig. 4. With the model, in a  $128 \times 64$  domain, at Reynolds numbers reduced by a factor of 2 due to cross-stream resolution effects, turbulence usually decayed through irregularly shaped patches, more rarely through streamwise or spanwise bands, exceptionally through oblique bands [17], which was attributed to a strong effect of the in-plane periodic boundary conditions used. Here this feature seems systematic and the bands appear persistent at  $R = 330$ . The wavelengths imposed by the in-plane boundary conditions are somewhat different from the experimental ones ( $\lambda_x = 128$  and  $\lambda_z = 64$  instead of  $\lambda_x \simeq 110$  and  $\lambda_z$  varying from  $\simeq 85$  at  $R = 335$  to  $\simeq 50$  at  $R = 395$ , respectively [7]). Standard in the theory of pattern formation, confinement effects would then explain a shifted transition. Since the transition is observed at decreasing  $R$ , in the Ginzburg–Landau framework alluded to above, this would imply a threshold shifted toward smaller values of  $R$ , i.e. below the experimental value  $R_t \simeq 415$  and, by the same token, a weakened modulation at comparable values of  $R$ . The relation between the light intensity measurement [7] and the amplitude of the energy contained in the perturbation<sup>3</sup> is not obvious but this seems to be the case. This makes us confident that gathering empirical unconstrained data on that special turbulent state, in systems at least twice as large, will help us understand the underlying mechanism and subsequently to model it.

## 4 Concluding remarks

Subcritical systems are characterised by the coexistence of different regimes. In the lower part of the transitional range, laminar flow coexists with chaotic flow in limited regions of physical space (puffs of spots). Experiments taking place in spatially extended domains, we have offered a hopefully relevant interpretation of the statistics of the transition alternative to the well accepted approach in terms of chaotic transients, showing in particular that the divergence of local transient chaos lifetime was not necessary for sustained (but weak) turbulence understood as intermittent spatiotemporal chaos.

Now, considering the turbulent band/spiral regime as a genuine but specific turbulent regime, the emergence of the bands/spirals offers us an example of continuous (second-order) turbulent-turbulent transition, complementary to the discontinuous (first-order) transition well documented in the case of the von Kármán swirling flow [23] of interest to the turbulent dynamo problem. Understanding such examples of coherent collective

<sup>2</sup>B&T’s approach is also 3D but in a quasi-1D context with the direction perpendicular to the bands playing a special role.

<sup>3</sup>Here just the distance to the *base* flow, not the turbulent energy currently defined as the distance to the *mean* flow.

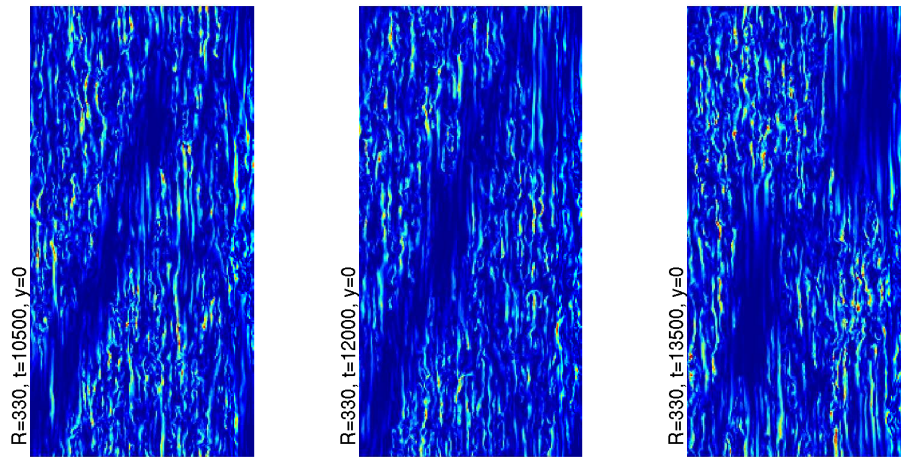


FIG. 4 – Oblique turbulent bands obtained in our simulations of the CHANNELFLOW program in an adiabatic  $R$  decrease experiment in a domain of size  $128 \times 2 \times 64$  ( $x$ -axis vertical). The perturbation energy  $\frac{1}{2}(u^2 + v^2 + w^2)$  in the mid-gap plane ( $x, 0, z$ ), is represented in color levels for times  $t = 10500$ ,  $12000$ , and  $13500$  after a sudden decrease of  $R$  from 350 to 330 at  $t = 9000$ ; see text.

behaviour in highly fluctuating environment is a strongly motivating perspective for on-going work.

## 5 Appendix : reduced model of plane Couette flow

Equations are written for the departure  $u, v, w, p$  from the base flow  $u_0 = y, v_0 = w_0 = 0, p_0 = \text{Cst.}$ . The first non-trivial correction is taken in the form :  $\{u, w\} = \{U_0, W_0\}B(1 - y^2) + \{U_1, W_1\}Cy(1 - y^2)$  and  $v = V_1A(1 - y^2)^2$ , where  $U_i, V_i, W_i$  are functions of  $x, z, t$ . The Galerkin projections of the momentum equations read :

$$\begin{aligned} \partial_t U_0 + N_{U_0} &= -\partial_x P_0 - a_1 \partial_x U_1 - a_2 V_1 + R^{-1}(\Delta - \gamma_0)U_0, \\ N_{U_0} &= \alpha_1(U_0 \partial_x U_0 + W_0 \partial_z U_0) + \alpha_2(U_1 \partial_x U_1 + W_1 \partial_z U_1 + \beta' V_1 U_1), \end{aligned}$$

and

$$\begin{aligned} \partial_t U_1 + N_{U_1} &= -\partial_x P_1 - a_1 \partial_x U_0 + R^{-1}(\Delta - \gamma_1)U_1, \\ N_{U_1} &= \alpha_2(U_0 \partial_x U_1 + U_1 \partial_x U_0 + W_0 \partial_z U_1 + W_1 \partial_z U_0 - \beta'' V_1 U_0), \end{aligned}$$

plus two similar equations governing  $W_0$  and  $W_1$  and an equation for  $V_1$  :

$$\partial_t V_1 + \alpha_3(U_0 \partial_x V_1 + W_0 \partial_z V_1) = -\beta P_1 + R^{-1}(\Delta - \gamma_1')V_1.$$

In these equations  $\Delta$  is the 2-dimensional Laplacian  $\partial_{x^2} + \partial_{z^2}$ . Explicit account of the pressure is avoided by defining  $\Psi_0, \Psi_1$ , and  $\Phi_1$  through  $U_0 = \bar{U}_0 - \partial_z \Psi_0$ ,  $W_0 = \bar{W}_0 + \partial_x \Psi_0$ ,  $U_1 = \bar{U}_1 + \partial_x \Phi_1 - \partial_z \Psi_1$ ,  $W_1 = \bar{W}_1 + \partial_z \Phi_1 + \partial_x \Psi_1$ , and  $\beta V_1 = \Delta \Phi_1$ , so that the Galerkin projections of the continuity condition are automatically fulfilled but the mean values  $\bar{U}_0, \dots$  need to be introduced and solved separately. These contributions to the flow are governed by

$$\frac{d}{dt} \bar{U}_0 = \alpha_2(\beta - \beta') \bar{U}_1 \bar{V}_1 - \gamma_0 R^{-1} \bar{U}_0 \quad \text{and} \quad \frac{d}{dt} \bar{U}_1 = \alpha_2(\beta + \beta'') \bar{U}_0 \bar{V}_1 - \gamma_1 R^{-1} \bar{U}_1.$$

and similar equations for  $\bar{W}_0, \bar{W}_1$ . The complete set, values of coefficients, and derived equations for  $\Psi_0, \Psi_1$  and  $\Phi_1$  can be found in [17].

## Acknowledgements

The members of the GIT at Saclay should be collectively thanked for the communication of their results and fruitful discussions. At LadHyX, M. Lagha played an important role in the development of the reduced model used in §2. We also thank Y. Duguet for discussions and communication of unpublished results. Finally, P.M. is particularly indebted to H. Chaté for his contribution to the interpretation of the statistics of laminar domains using that model. Simulations were performed thanks to CPU time allocations of IDRIS (Orsay) under projects #61462 and #72138.

## Références

- [1] Eckhardt B., Faisst H., Schmiegel A., and Schneider T. Dynamical systems and the transition to turbulence in linearly stable shear flows. *Phil. Trans. R. Soc. A*, 366, 1297–1315, 2008.
- [2] Hof B., de Lozar A., Kuik D., and Westerweel J. Repeller or attractor ? selecting the dynamical model for the onset of turbulence in pipe flow. *Phys. Rev. Lett.*, 101, 214501.1–4, 2008.
- [3] Willis A., Peixinho J., Kerswell R., and Mullin T. Experimental and theoretical progress in pipe flow transition. *Phil. Trans. R. Soc. A*, 366, 2671–2684, 2008.
- [4] Hof B., Westerweel J., Schneider T., and Eckhardt B. Finite lifetime of turbulence in shear flows. *Nature*, 443, 59–62, 2006.
- [5] Bottin S., Daviaud F., Manneville P., and Dauchot O. Discontinuous transition to spatiotemporal intermittency in plane Couette flow. *Europhys. Lett.*, 43, 171–176, 1998.
- [6] Pomeau Y. Front motion, metastability and subcritical bifurcations in hydrodynamics. *Physica D*, 23, 3–11, 1986.
- [7] Prigent A. La spirale turbulente : motif de grande longueur d’onde dans les écoulements cisailés turbulents. PhD thesis, Université Paris-Sud, Orsay, 2001.
- [8] Prigent A., Grégoire G., Chaté H., and Dauchot O. Long-wavelength modulation of turbulent shear flows. *Physica D*, 174, 100–113, 2003.
- [9] Faisst H. and Eckhardt B. Sensitive dependence on initial conditions in transition to turbulence in pipe flow. *J. Fluid Mech.*, 504, 343–352, 2004.
- [10] Viswanath D. Recurrent motions within plane Couette flow. *J. Fluid Mech.*, 580, 339–358, 2007.
- [11] Tsukahara T., Kawamura H., and Shingai K. DNS of turbulent Couette flow with emphasis on the large-scale structure in the core region. *J. of Turbulence*, 7, 19.1–16, 2006.
- [12] Schlatter P., Duguet Y., and Henningson D. Plane Couette flow simulations. private communication of Y. Duguet, 2009.
- [13] Barkley D. and Tuckerman L. Computational study of turbulent laminar patterns in Couette flow. *Phys. Rev. Lett.*, 94, 014502.1–4, 2005.
- [14] Barkley D. and Tuckerman L. Mean flow of turbulent-laminar patterns in plane Couette flow. *J. Fluid Mech.*, 576, 109–137, 2007.
- [15] Bottin S. and Chaté H. Statistical analysis of the transition to turbulence in plane Couette flow. *Eur. Phys. J. B*, 6, 143–155, 1998.
- [16] Manneville P. and Locher F. A model for transitional plane Couette flow. *C.R. Acad. Sci. Paris*, 328 Série IIb, 159–164, 2000.
- [17] Lagha M. and Manneville P. Modeling transitional plane Couette flow. *Eur. Phys. J B*, 58, 433–447, 2007.
- [18] Mullin T. and Kerswell R. IUTAM Symposium on Laminar-Turbulent Transition and Finite Amplitude Solutions. Springer, 2005.
- [19] Waleffe F. On a self-sustaining process in shear flows. *Phys. Fluids*, 9, 883–900, 2004.
- [20] Manneville P. Spatiotemporal perspective on the decay of turbulence in wall-bounded flows. *Phys. Rev. E*, 79, 025301.1–4 (R) [and erratum to appear], 2009.
- [21] Lagha M. and Manneville P. Large scale flow around turbulent spots. *Phys. Fluids*, 19, 094105.1–9, 2007.
- [22] Gibson J. Channelflow : a spectral navier-stokes simulator in c++  
<http://www.cns.gatech.edu/channelflow/>, 1999–200x.
- [23] Ravelet F., Marié L., Chiffaudel A., and Daviaud F. Multistability and memory effects in a highly turbulent flow : experimental evidence for a global bifurcation. *Phys. Rev. Lett.*, 93, 164501.1–4, 2004.